

The crystal structure of 1,2,3,4,6-*penta*-*O*-benzoyl- α -D-mannopyranose: observation of C–H $\cdots\pi$ interaction as a surrogate to O–H \cdots O interaction of a free sugar

B. Muktha,^a O. Srinivas,^b M.R. Amresh,^b T.N. Guru Row,^{a,*} N. Jayaraman,^{b,*} K. Sekar^c

^a Solid State and Structural Chemistry Unit, Indian Institute of Science, Bangalore 560 012, India

^b Department of Organic Chemistry, Indian Institute of Science, Bangalore 560 012, India

^c Bioinformatics Center, Indian Institute of Science, Bangalore 560 012, India

Received 12 June 2003; received in revised form 10 July 2003; accepted 13 July 2003

Abstract

The crystal structure of the title compound was determined by X-ray crystallography. The compound crystallized in the orthorhombic space group $P2_12_12_1$ with four molecules in the unit cell with $a = 9.170(2)$, $b = 9.873(2)$, $c = 38.831(8)$ Å. The structure was refined to a R index of 0.041 for 7907 independent reflections. The mannopyranose unit adopts a distorted 4C_1 conformation. The structure depicts unique network of C–H $\cdots\pi$ interactions, very closely resembling the pattern of O–H \cdots O interactions in free sugars. This intriguing and rare observation points to a notion that the supramolecular organization pertaining to a sugar is in-built in the pyranose ring itself.

© 2003 Elsevier Ltd. All rights reserved.

Keywords: Conformation; Crystal structures; C–H $\cdots\pi$ interaction; Hydrogen bonding; α -D-Mannose; Pyranose

1. Introduction

The OH \cdots O type hydrogen bonding is the most prevalent non-covalent force that accounts for the stability, molecular conformation and packing of hydroxyl group abundant carbohydrates.^{1,2} The nature of supramolecular organization arising from OH \cdots O hydrogen bonds in free sugars was studied systematically by Jeffrey and co-workers³ and the most important outcome of these studies⁴ is the recognition of certain general patterns as: (1) all the available hydroxyl groups and as many as of the ring and the glycosidic oxygens take part in the hydrogen bonding; (2) there is a cooperativity in forming infinite or long finite hydrogen bonds; and (3) the anomeric hydroxyl group and the ring oxygen are weak hydrogen bond acceptors and tend to function as ‘chain stoppers’. Among the many

complex interactions possible, hydrogen bonding is by far the most studied and well understood.⁵ The preference to well defined geometrical arrangements in the crystalline lattice is a property of the O–H \cdots O type of hydrogen bonds, especially in carbohydrates.⁴ It is of interest to inquire whether the inherent control of the hydrogen bonding network by the sugar ring is preserved in derivatives not possessing the OH \cdots O type hydrogen bonding possibilities. In this context, we have determined the crystal structure of the title compound **1** (Fig. 1), containing five benzoate groups on the molecular periphery, which facilitates well defined, weak but highly directional C–H $\cdots\pi$ interactions. The C–H $\cdots\pi$ interaction can be regarded as the weakest extreme of hydrogen bonds, which occurs between CH groups (soft acids) and π systems (soft bases).⁶ The substituent effect on conformational equilibria,^{7,8} crystal packing⁹ and equilibrium of supramolecular complexes¹⁰ demonstrate that the C–H $\cdots\pi$ interaction is not merely a conventional van der Waals force but has a hydrogen bond-like property. The enthalpy of a single unit of C–H $\cdots\pi$ interaction is around 1 kcal mol^{−1}.^{11,12}

* Corresponding author. Tel.: +91-80-2832578, +91-80-2932403; fax: +91-80-3600529.

E-mail address: jayaraman@orgchem.iisc.ernet.in (N. Jayaraman).

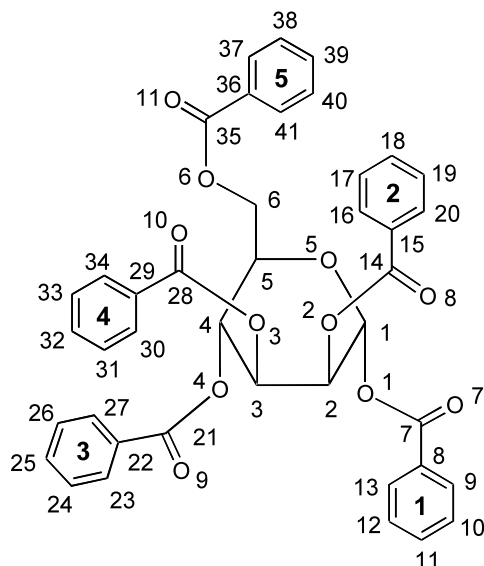


Fig. 1. Molecular structure of **1**. Hydrogen atoms are omitted for clarity. The number inside the aromatic rings denotes its position at a particular pyranose ring carbon atom.

It is well recognized that C–H··· π interaction plays a crucial part in controlling the crystal packing of organic molecules.^{13–15} Despite broad interests in the C–H··· π interaction in many areas of chemistry and biology, very little is known about such a non-covalent interaction in carbohydrates. Herein we report the first instance of the crystal structure of 1,2,3,4,6-*penta-O*-benzoyl- α -D-mannopyranose stabilized mainly by C–H··· π interactions.

2. Experimental

Perbenzoylation of α -D-mannose to **1** (Fig. 1) was performed according to the reported procedure.¹⁶ Colorless and transparent crystals of **1** were obtained by slow evaporation from a 1:1 mixture of CH_2Cl_2 and hexane. A suitable crystal of size (0.313 \times 0.252 \times 0.095 mm) was checked for extinction under a polarizing microscope and then mounted on a Bruker AXS Smart Apex CCD diffractometer¹⁷ with a crystal to detector distance of 6.03 cm. Compound **1** crystallizes in the orthorhombic space group $P2_12_12_1$ with four molecules in the unit cell with $a = 9.170(2)$, $b = 9.873(2)$, $c = 38.831(8)$ Å. A total of 7907 independent reflections were measured with monochromatic Mo K_α radiation ($\lambda = 0.7107$ Å, 50 KV, 35 mA). The data were reduced using Saint Plus¹⁷ and the structure was solved by direct methods and refined using SHELXL,¹⁸ to $R = 0.041$, $wR = 0.089$ and $S = 0.963$. All the non-hydrogen atoms were treated anisotropically and the hydrogen atoms were located using difference Fourier techniques and were also refined isotropically. The crystallographic data is summarized in Table 1.

Table 1
Experimental details

<i>Crystal data</i>	
Chemical formula	$\text{C}_{41}\text{H}_{34}\text{O}_{11}$
Chemical formula weight (M_r)	700.7
Temperature (K)	293
Cell setting	orthorhombic
Space group	$P2_12_12_1$
a, b, c (Å)	9.169 (1), 9.873 (2), 38.831(8)
V (Å ³)	3515.49(13)
Z	4
D_x (mg m ^{−3})	1.32
Crystal size (mm)	0.31 \times 0.25 \times 0.09
θ Range (°)	2.10–55.74
No. of reflections for cell parameters	7907
Radiation type	Mo K_α radiation
Crystal form, colour	Block, white
<i>Data collection</i>	
Diffractometer	SMART APEX CCD area detector
Data collection method	ϕ scan
No. of measured, independent and observed reflections	389079, 7907 and 5424
Criterion for observed reflections	$I > 2\sigma(I)$
R_{int}	0.043
θ_{max} (°)	55.74
Range of h, k, l	−11 \rightarrow 11, −12 \rightarrow 12, −50 \rightarrow 50
Absorption correction	SADABS
Extinction correction	None
<i>Refinement</i>	
Refinement on	F^2
R, wR, S	0.041, 0.089, 0.963
No. of reflections and parameters used in refinement	7907 and 517
H-atom treatment	Refined independently
Weighting scheme	$w = 1/\sigma^2(F_o^2)$
$\Delta\rho_{\text{max}}, \Delta\rho_{\text{min}}$ (e Å ^{−3})	0.140, −0.121

3. Results and discussion

An ORTEP diagram of **1** is shown in Fig. 2 and the packing of the molecules in the crystal lattice is illustrated in Fig. 3. All significant bond distances and bond angles are given in Table 2. Torsion angles pertaining to the pyranose ring are given in Table 3. The observed C–H··· π interactions in the packing motif are given in Table 4.

The C–C bond lengths within the pyranose ring have bond lengths ranging between 1.522 and 1.530 Å. The *endocyclic* O5–C1 bond length of 1.398(2) Å is found to be the shortest in the pyranose ring. The bond lengths C5–O5 and C1–O1 are 1.431(2) and 1.425(2) Å, respectively. The shortening of O5–C1 bond compared

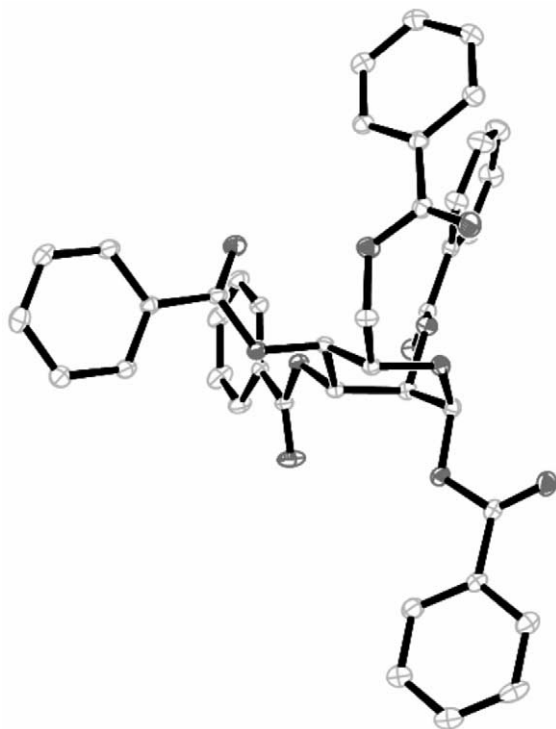


Fig. 2. ORTEP of **1** with the displacement ellipsoids at 10% probability level. Atom numbering is omitted for clarity. The atom numbers of this ORTEP diagram can be related from Fig. 1.

Table 2

Selected bond lengths and bond angles (estimated standard deviations in parentheses)

Bond	Length (Å)	Bonds	Angle (°)
O5–C1	1.3976 (25)	O1–C1–O5	111.69 (0.16)
C2–C1	1.5222 (29)	O2–C2–C1	103.61 (0.15)
C3–C2	1.5139 (28)	C2–C3–C4	109.96 (0.17)
C3–C4	1.5028 (28)	C5–C4–C3	110.39 (0.16)
C5–C4	1.5313 (28)	C2–C1–H1	111.01 (1.26)
O5–C5	1.4313 (23)	O1–C1–H1	108.72 (1.26)
C1–H1	0.8953 (201)	O1–C7–O7	122.03 (0.21)
O1–C1	1.4249 (26)	C3–C2–C1	111.12 (0.17)
O1–C7	1.3672 (25)	C2–O2–C14	117.58 (0.15)
C2–H2	0.9822 (201)	C5–O5–C1	114.25 (0.15)
O2–C2	1.4412 (24)	O2–C14–O8	123.23 (0.18)
O2–C14	1.3513 (24)	C2–C3–H3	110.69 (0.97)
C3–H3	1.0316 (174)	O3–C3–H3	108.42 (0.98)
O3–C3	1.4381 (24)	C3–O3–C21	116.58 (0.15)
O3–C21	1.3479 (24)	O3–C21–O9	122.94 (0.19)
O4–C4	1.4330 (23)	O3–C3–C4	107.05 (0.15)
C4–H4	0.8963 (166)	O4–C4–C3	110.38 (0.16)
O4–C28	1.3527 (24)	O4–C4–H4	111.45 (1.04)
C5–C6	1.5055 (30)	O4–C28–O10	122.46 (0.20)
C5–H5	1.009 (192)	O4–C4–C5	106.73 (0.15)
C6–H6B	1.0371 (244)	O5–C5–C6	107.32 (0.17)
C6–H6A	0.9453 (225)	O6–C6–C5	109.69 (0.18)
O6–C6	1.4385 (28)	C35–O6–C6	119.19 (0.18)
O6–C35	1.3296 (28)		

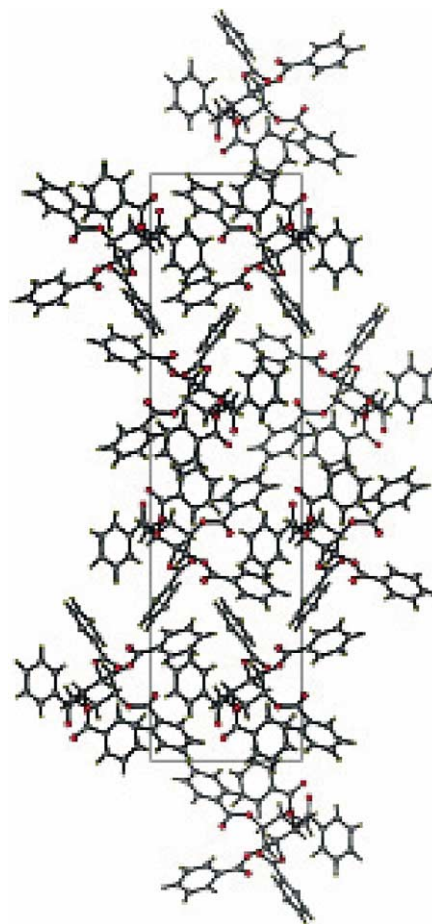


Fig. 3. Packing of **1** viewed along *a* axis.

to C1–O1 bond distance indicates that there is no significant anomeric effect, which is normally found in free sugar derivatives.¹⁹ It appears that the lone pair of electrons of O5 interact with the antibonding orbital of *exocyclic* C1–O1 bond, which will account not only the lengthening of C1–O1 bond, but also the shortening of O5–C1 bond. The bond lengths of the benzoate units are similar with a mean bond length of O–C 1.349; C=O 1.195; CO–C (aromatic) 1.480 Å, respectively. Also, there is no unusual deviation for the pyranose ring angles (range between 107.3 and 114.3°).

The molecular conformation of **1** correlates well with the parent compound α -D-mannose.²⁰ The valence bond angles in the sequence C5–O5–C1–O1 are 114.3 and 111.7°, respectively, indicate the α configuration of the substituent at the anomeric center. The molecular conformation is 4C_1 with Cremer–Pople puckering parameter²¹ $Q = 0.547$ Å, $\theta = 176.8^\circ$ and $\varphi = 75.4^\circ$ and these parameters indicate that there is a slight distortion of the ring from the ideal chair conformation, for which $\theta = 0$ or 180° , $\varphi = 0^\circ$ and $Q \sim 0.55$ Å and is towards the skew conformation.^{22–24} The torsion angles O5–C5–C6–O6 of $+75.7^\circ$ and C4–C5–C6–O6 of -45.7° indicate the *gauche*–*gauche* orientation of primary

Table 3
Selected torsion angles (estimated standard deviations in parantheses)

Pyranose ring	Angle (°)
O5–C5–C4–O4	176.38 (0.14)
O5–C5–C4–C3	56.40 (0.20)
O5–C1–O1–C7	–83.4 (0.21)
C6–C5–C4–O4	–63.80 (0.21)
C6–C5–C4–C3	176.22 (0.17)
O5–C5–C6–O6	75.73 (0.20)
C4–C5–C6–O6	–45.72 (0.23)
C1–O5–C5–C4	–58.24 (0.20)
C1–O5–C5–C6	178.75 (0.17)
C5–O5–C1–O1	–62.98 (0.21)
C5–O5–C1–C2	56.68 (0.21)
O3–C3–C2–O2	55.92 (0.20)
O3–C3–C2–C1	169.49 (0.16)
C4–C3–C2–O2	–61.45 (0.20)
C4–C3–C2–C1	52.12 (0.22)
O3–C3–C4–O4	69.06 (0.19)
O3–C3–C4–C5	–173.19 (0.15)
C2–C3–C4–O4	–172.03 (0.15)
C2–C3–C4–C5	–54.27 (0.21)
C2–C1–O1–C7	153.8 (0.17)
O2–C2–C1–O1	–173.34 (0.15)
O2–C2–C1–O5	64.11 (0.20)
C3–C2–C1–O1	69.75 (0.21)
C3–C2–C1–O5	–52.80 (0.22)

benzoyloxy group with respect to the ring oxygen as well as to the C-4 substituent. On the other hand, the torsion angles of C7–O1–C1–O5 of -83.4° and C7–O1–C1–C2 of 153.8° show that the anomeric substituent has *gauche*–*trans* orientation with respect to the pyranose ring. The ester group conformation shows that the bond CO–COPh is nearly antiparallel and deviates from 180° by a value of 3.3 (C1), 2.5 (C2), 11.6 (C3), 8.2 (C4) and 5.5° (C6), respectively. The bond length of O1–C7 is 1.367 Å, which is the highest when compared to other O–C bonds in the pyranose (O2–C14, O3–C21, O4–C28 and O6–C35; mean bond length = 1.346 Å). The

lengthening of O1–C7 bond is likely to arise due the attachment of benzoyl group at O1 position of the anomeric center.

The most interesting result from the structural analysis is the non-covalent bonding responsible for the packing in the crystal structure. The molecular packing is fully dominated by C–H $\cdots\pi$ interactions, involving all the aromatic rings and only two hydrogen atoms H5 and H6a from the sugar moiety. The approach suggested by Nishio and co-workers²⁵ has been employed to analyze the rather complex network of C–H $\cdots\pi$ interactions (Fig. 4, Table 4). The interaction has been classified based on the approach distance of the hydrogen atom to the plane and the orientation of the plane with respect to the C–H bond. The C–H $\cdots\pi$ contacts have been identified using PARST97.²⁶ An intermolecular distance [D_{\max} 3.05; 2.9 Å for C–H plus 1.7 Å for a half thickness of the aromatic ring) \times 1.05] was considered to be relevant for the presence of a C–H $\cdots\pi$ interaction. An examination of the interactions shows that the D_{lin} which represents the distance between the H atom of the C–H moiety with the midpoint of the closest aromatic C–C bond is either closer to or shorter than D_{\max} . The values of D_{pln} , the distance between the C–H moiety and the centroid of the aromatic ring, were found to be higher than D_{\max} . Such features have been analyzed²⁷ and it has been established based on accurate X-ray and neutron experiments that the directionality is important for representing these weak interactions.

The geometric parameters of the C–H $\cdots\pi$ interactions in the crystal are given in Table 4. There are seven well-defined C–H $\cdots\pi$ interactions, among these, four of the five aromatic rings display both donor and acceptor character with respect to the hydrogen atoms involved in these interactions. Also, these interactions can be classified into two categories, one infinite C–H $\cdots\pi$ interaction constituted by aromatic groups at positions 3 and 4 of the pyranose ring and another finite C–H $\cdots\pi$ interaction along the *c* axis, which involves the rest of aromatic rings at positions 1, 2 and 5 of the pyranose

Table 4
Intermolecular C–H $\cdots\pi$ interactions

Interaction	D_{atm} (Å)	D_{lin} (Å)	θ (°)	ω (°)	Label
C(5)H(5) \cdots C(24)	3.047	3.184	27.29	97.60	Sugar 5-H \cdots 3 π
C(32)H(32) \cdots C(23)	2.987	3.063	42.15	104.88	4-H _{para} \cdots 3 π
C(33)H(33) \cdots C(30)	2.902	3.062	31.11	109.63	4-H _{meta} \cdots 4 π
C(27)H(27) \cdots C(34)	2.942	2.956	23.08	105.1	3-H _{ortho} \cdots 4 π
C(38)H(38) \cdots C(12)	2.984	2.971	36.22	124.82	5-H _{meta} \cdots 1 π
C(41)H(41) \cdots C(20)	2.920	2.991	42.23	92.8	5-H _{ortho} \cdots 2 π
C(6)H(6a) \cdots C(17)	2.963	3.043	17.55	93.32	Sugar 6-Ha \cdots 2 π

Symmetry Code: (1) x , $+y+1$, $+z$; (2) $-x+1$, $+y+1/2$, $-z+1/2$; (3) $-x+1$, $+y+1/2$, $-z+1/2$; (4) $x+2$, $+y-1/2$, $-z+1/2$; (5) $-x+1$, $+y+1/2$, $-z+1/2$; (6) $x+1/2$, $-y+1/2$, $-z$; (7) x , $+y+1$, $+z$.

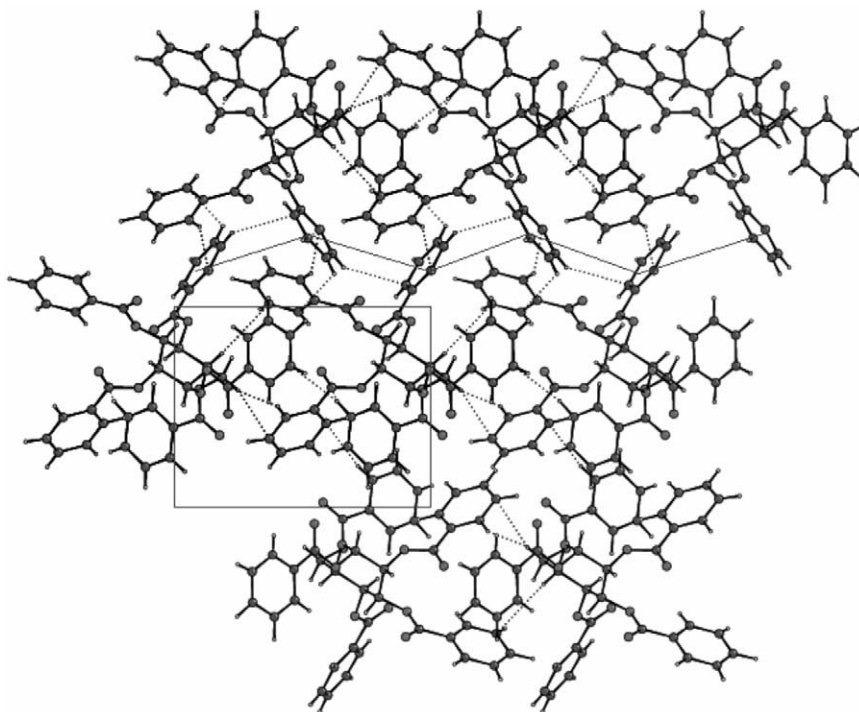


Fig. 4. C–H \cdots π interactions: the zig-zag line indicates the infinite chain and the dotted lines indicate the finite interactions.

ring (Fig. 4). In the infinite C–H \cdots π interaction, the role of aromatic ring 4 is anomalous: while the *meta* hydrogen (4-H_{meta}) interacts with the 4 π -orbital of another molecule, the adjacent *para* hydrogen (4-H_{para}) interacts with the π -orbital of aromatic ring 3. The aromatic ring 3 in turn acts as both donor and acceptor to bridge the aromatic ring 4 between the adjacent layers. A stereoview of this infinite C–H \cdots π interaction is shown in Fig. 5. The involvement of the *meta* and *para* hydrogens as well as the π -orbital of aromatic ring 4 as two-point donor and two-point acceptor is intriguing and is a feature of this infinite C–H \cdots π interaction. On the other hand, in the finite C–H \cdots π interactions the nature of C–H \cdots π connectivity is 3- π \cdots Sugar5-H—Sugar6-Ha \cdots 2- π \cdots 5-H_{ortho}—5-H_{meta} \cdots 1- π (Fig. 6). This implies the involvement of five individual molecules along the 2₁ screw axis to generate this finite chain. Also, the aromatic ring 3 connects the

infinite and finite chains, which are perpendicular to each other. An optimum geometry of the finite interaction also requires the sugar H-5 and H-6a as hydrogen donors, which lead to a ‘sugar bend’ due to the presence of both of these donors arising from the same molecule (Fig. 6). The finite chain terminates at aromatic ring 1, which acts as a π -acceptor. Along the *c* axis, the finite chains interpenetrate completely, resulting in a dense packing of the molecules. The layers of infinite chains are at a distance of 19.9 Å from the finite chains and the screw axial symmetry in all three directions results in a network of the C–H \cdots π interactions.

It is pertinent to compare these results with the more robust OH \cdots O hydrogen bonding pattern that exist in free OH groups containing pyranoses and pyranosides.⁴ The general patterns of OH \cdots O hydrogen bonding interactions corresponding to a free sugar (*vide supra*) appear to be valid even in the case of weaker C–H \cdots π

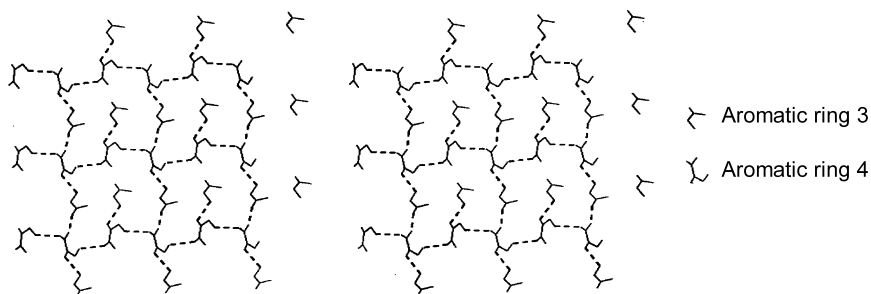


Fig. 5. Stereoview of infinite CH \cdots π interactions arising from aromatic rings 3 and 4. The fragments corresponding to the CH \cdots π interaction distance between these two aromatic rings as given in Table 4 are used to generate the view.

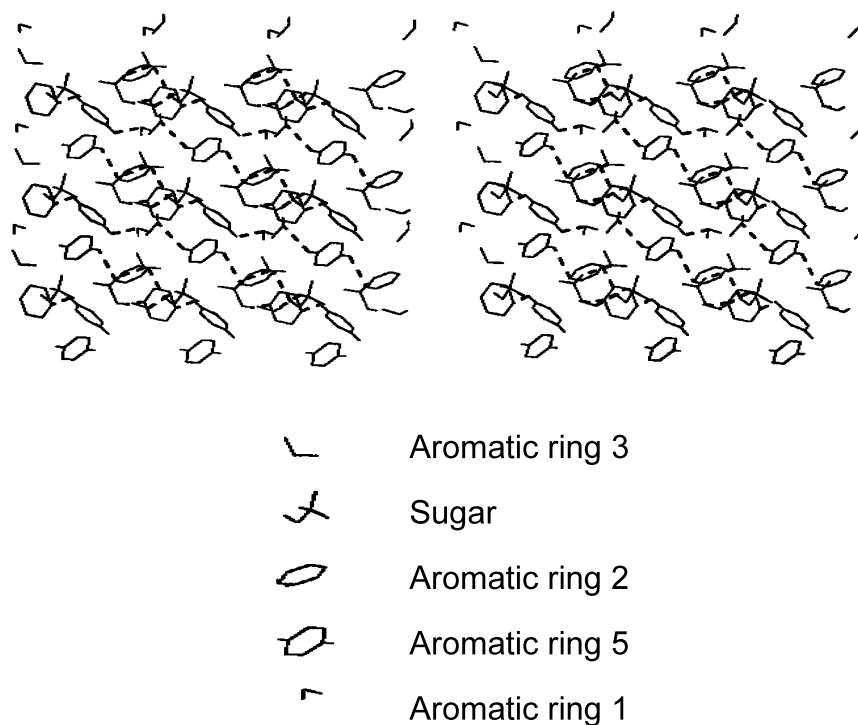


Fig. 6. Stereoview of finite $\text{CH}\cdots\pi$ interactions arising from aromatic rings 1, 2, 3, 5 and the sugar unit of **1**. The fragments corresponding to the $\text{CH}\cdots\pi$ interaction distance between these aromatic rings and the sugar unit as given in Table 4 are used to generate the view.

interactions, namely: (i) all the available aromatic rings of benzoyl groups take part in the $\text{C}-\text{H}\cdots\pi$ interactions; (ii) there is a co-operativity in forming both infinite or long finite $\text{C}-\text{H}\cdots\pi$ interactions; and (iii) the aromatic ring attached to the anomeric position act as a 'chain stopper' of the long finite $\text{C}-\text{H}\cdots\pi$ interaction. The results of the structural analysis are unique in at least two accounts: (i) it clearly demonstrates that the exclusive $\text{C}-\text{H}\cdots\pi$ interactions alone can play an important role in controlling the crystal packing; and (ii) the generalized rules of crystal packing in cyclic sugar structures does not appear to be limited to $\text{O}-\text{H}\cdots\text{O}$ hydrogen bonding, but it can be extended to other types of interactions also, that of $\text{C}-\text{H}\cdots\pi$ interactions in the present report. Upon Cambridge Structural Database search (CSD, CONQUEST Version 1.4, with 2.5 lakh entries), we also find that the present report stands first for the single crystal X-ray determination of a perbenzoylated pyranose sugar and thus precluding the possibility for comparison with similar structures. It is very likely that the non-covalent bonding forces follow a nearly rigid pattern that is characteristic of sugar structures in general. An exclusive $\text{C}-\text{H}\cdots\pi$ interaction alone can fulfill such a rigid pattern, similar to $\text{OH}\cdots\text{O}$ interactions of free sugars, is shown for the first time in a cyclic sugar structure.

4. Supplementary material

The data were deposited at the Cambridge Structural database (Accession number CCDC 197033). Copies of this information can be obtained free of charge from The Director, CCDC, 12 Union Road, Cambridge CB2 1EZ, UK (fax: +44-1223-336033; e-mail: deposit@ccdc.cam.ac.uk or <http://www.ccdc.cam.ac.uk>).

Acknowledgements

We thank Department of Science and Technology, India for data collection on the CCD facility setup under the IRFA-DST program. NJ thanks Third World Academy of Sciences, Trieste, Italy, for a partial financial support and Professor K. Venkatesan for helpful discussions.

References

1. Jeffrey, G. A.; Saenger, W. *Hydrogen Bonding in Biological Structures*; Springer: Berlin, 1991.
2. Steiner, T.; Saenger, W. *Carbohydr. Res.* **1994**, 259, 1–12.
3. Ceccarelli, C.; Jeffrey, G. A.; Taylor, R. *J. Mol. Struct.* **1981**, 70, 255–271.

4. Jeffrey, G. A.; Mitra, J. *Acta Crystallogr.* **1983**, B39, 469–480.
5. Desiraju, G. R.; Steiner, T. *The Weak Hydrogen Bond in Structural Chemistry and Biology*; Oxford University Press: Oxford, 1999.
6. Nishio, M.; Hirota, M.; Umezawa, Y. *The CH/π Interaction: Evidence, Nature and Consequences*; Wiley-VCH: New York, 1998.
7. Kishikawa, K.; Yoshizaki, K.; Kohmoto, S.; Yamamoto, M.; Yamaguchi, K.; Yamada, K. *J. Chem. Soc. Perkin Trans. 1* **1997**, 1233–1240.
8. Suezawa, H.; Hashimoto, T.; Tsuchinaga, K.; Yoshida, T.; Yuzuri, T.; Sakakibara, K.; Hirota, M.; Nishio, M. *J. Chem. Soc. Perkin Trans. 2* **2000**, 1243–1249.
9. Madhavi, N. N. L.; Katz, A. K.; Carrell, H. L.; Nangia, A.; Desiraju, G. R. *Chem. Commun.* **1997**, 1953–1954.
10. Kobayashi, K.; Asakawa, Y.; Aoyama, Y. *Supramol. Chem.* **1993**, 2, 133.
11. Tsuzuki, S.; Honda, K.; Uchamaru, T.; Mikami, M.; Tanabe, K. *J. Am. Chem. Soc.* **2000**, 122, 3746–3753.
12. Kim, E. I.; Paliwal, S.; Wilcox, C. S. *J. Am. Chem. Soc.* **1998**, 120, 11192–11193.
13. Steiner, T. *J. Chem. Soc. Chem. Commun.* **1995**, 95–96.
14. Hunter, C. A.; Lawson, K. R.; Perkins, J.; Urch, C. J. *J. Chem. Soc. Perkin Trans. 2* **2001**, 651–669.
15. Umezawa, Y.; Tsubuyama, S.; Honda, K.; Uzawa, J.; Nishio, M. *Bull. Chem. Soc. Jpn.* **1998**, 71, 1207–1213.
16. Ness, R. K.; Fletcher, H. G., Jr.; Hudson, C. S. *J. Am. Chem. Soc.* **1950**, 72, 2200–2205.
17. Bruker SMART and SAINT. Bruker AXS Inc., Madison, Wisconsin, USA, **1998**.
18. Sheldrick, G.M. SHELXS97 and SHELXL97. University of Göttingen, Germany, **1997**.
19. Berman, H. M.; Chu, S. S. C.; Jeffrey, G. A. *Science* **1967**, 157, 1576–1577.
20. Longchambon, F.; Neuman, A. *Acta Crystallogr.* **1976**, B32, 1822–1826.
21. Cremer, D.; Pople, J. A. *J. Am. Chem. Soc.* **1975**, 97, 1354–1358.
22. Jeffrey, G. A. *Acta Crystallogr.* **1990**, B46, 89–103.
23. Jeffrey, G. A.; Yates, J. H. *Carbohydr. Res.* **1979**, 74, 319–322.
24. Stoddart, J. F. *Stereochemistry of Carbohydrates*; Wiley: New York, 1971.
25. Takahashi, H.; Tsuboyama, S.; Umezawa, Y.; Honda, K.; Nishio, M. *Tetrahedron* **2000**, 56, 6185–6191.
26. Nardelli, L. J. *Appl. Crystallogr.* **1995**, 28, 659.
27. Broder, C. K.; Howard, J. A. K.; Keen, D. A.; Wilson, C. C.; Allen, F. H.; Jetti, R. K. R.; Nangia, A.; Desiraju, G. R. *Acta Crystallogr.* **2000**, B56, 1080–1084.